







Proceedings Article

# A Denoiser Scaling Technique for Plug-and-Play MPI Reconstruction

Alper Güngör <sup>a,b,\*</sup>. Baris Askin <sup>a,c</sup>. Damla Alptekin Soydan <sup>b</sup>. Emine Ulku Saritas <sup>a,d</sup>.  
Can Barış Top <sup>b</sup>. Tolga Çukur <sup>a,d</sup>

<sup>a</sup>Department of Electrical and Electronics Engineering, Bilkent University, Ankara, Turkey

<sup>b</sup>Aselsan Research Center, Ankara, Turkey

<sup>c</sup>Department of Electrical and Computer Engineering, Carnegie Mellon University, Pittsburgh, PA, USA

<sup>d</sup>National Magnetic Resonance Research Center (UMRAM), Bilkent University, Ankara, Turkey

\*Corresponding author, email: [alperg@ee.bilkent.edu.tr](mailto:alperg@ee.bilkent.edu.tr)

© 2023 Güngör *et al.*; licensee Infinite Science Publishing GmbH

This is an Open Access article distributed under the terms of the Creative Commons Attribution License (<http://creativecommons.org/licenses/by/4.0>), which permits unrestricted use, distribution, and reproduction in any medium, provided the original work is properly cited.

## Abstract

Image reconstruction based on the system matrix in magnetic particle imaging (MPI) involves an ill-posed inverse problem, which is often solved using iterative optimization procedures that use regularization. Reconstruction performance is highly dependent on the quality of information captured by the regularization prior. Learning-based methods have been recently introduced that significantly improve prior information in MPI reconstruction. Yet, these methods can perform suboptimally under drifts in the image scale between the training and test sets. In this study, we assess the influence of scale drifts on the performance a recent plug-and-play method (PP-MPI) that uses a pre-trained denoiser. We introduce a new denoiser scaling technique that improves reliability of PP-MPI against deviations in image scale. The proposed technique enables high quality reconstructions that are robust against scale drifts between training and testing sets.

## 1. Introduction

Magnetic particle imaging (MPI) allows high resolution and contrast imaging of magnetic nanoparticles (MNP). A common framework for image reconstruction poses an inverse problem based on the system matrix (SM) [1], which can then be solved using regularized, iterative optimization. Because the inverse problem is ill-posed, reconstruction quality relies heavily on the regularization prior. Conventional methods usually employ hand-designed priors such as  $\ell_2$ -norm or a linear combination of  $\ell_1$ -norm and total variation [2, 3].

Recent studies have proposed learning-based methods that improve reconstruction performance [4–8]. These methods learn a data-driven prior based on the distribution of images in a training set. Therefore, distri-

butional drifts encountered at test time can compromise their performance. A common drift in MPI pertains to the native changes in image scale [9]. Characterizing the sensitivity of learning-based methods to scale drifts is critical for their adoption, and improved techniques are needed to ensure reliability against scale drifts.

Here, we assess the sensitivity to image scale in a plug-and-play method, PP-MPI, that we recently introduced for MPI reconstruction [9]. PP-MPI trains a deep residual architecture to denoise synthetic MPI image, then uses this denoising prior to regularize the solution of an iterative optimization that reconstructs actual MPI image. To enhance reliability against scale drifts, we propose a new denoiser scaling technique for MPI reconstruction that does not include any tunable scale-dependent parameters. Our proposed technique performs a small number

of iterations to obtain an initial image for estimating the scaling parameter, and then scales the denoiser accordingly in remaining iterations. We compare the proposed technique to other non-scaled baselines that are trained on low-dynamic range (LDR), mid-dynamic range (MDR) and high-dynamic range (HDR) images, respectively. We show that the proposed technique outperforms all baselines under scale mismatch.

## II. Theory

SM-based reconstruction uses the linear forward model:

$$\mathbf{Ax} + \mathbf{n} = \mathbf{y}, \quad (1)$$

where  $\mathbf{A}$  is the SM,  $\mathbf{x}$  is the image vector,  $\mathbf{n}$  is the noise vector, and  $\mathbf{y}$  is the data vector.  $\mathbf{A}$  is often measured with a calibration scan [10]. The measured SM is then used to recover the images by solving an optimization [3]:

$$\arg \min_{\mathbf{x}} R(\mathbf{x}) \text{ s. t. } \|\mathbf{Ax} - \mathbf{y}\|_2 \leq \epsilon, \quad (2)$$

where  $R(\cdot)$  is the regularization prior and  $\epsilon$  is the error bound on the noise level. Conventional methods use hand-designed priors such as  $\ell_2$ -norm or a linear combination of  $\ell_1$ -norm and total variation for reconstruction. However, these priors may fall short of capturing intricate attributes of MPI images. As an alternative, learning-based methods based on multi-layer perceptron (MLP) [7, 8] and untrained convolutional neural network (CNN) models [4, 6] have been proposed. Data-driven models that are trained for a specific SM might show limited generalization, whereas learning untrained models at test time can yield high computational burden.

We have recently proposed a plug-and-play method for MPI (PP-MPI) [9]. PP-MPI uses a dense residual architecture that is pre-trained to perform a denoising task on noise-added MPI phantoms, derived synthetically from experimental magnetic resonance angiogram (MRA) images. During reconstruction with an iterative optimization, the image is projected through the trained network for regularization (see Alg. 1). While promising results have been reported with PP-MPI, its performance is affected by scale drifts between training and test images. Here, we propose a new technique for improving the robustness of PP-MPI against mismatches between the dynamic ranges of training versus test images. The proposed technique performs few iterations with the pre-trained, non-scaled denoiser to obtain an initial estimate of the image scale. Denoiser scaling is then performed based on this estimate in remaining iterations, to address the scale drift between the training-test sets [11]. Here, the scaling parameter  $\gamma$  is taken as the peak image intensity after 40 iterations, and denoiser scaling is then achieved by normalizing the denoiser input and multiplying the denoised image by  $\gamma$ :

$$\mathbf{z}_{n+1}^{(1)} = \gamma f_{PP}(1/\gamma(\mathbf{x}_{n+1} - \mathbf{d}_n^{(1)})). \quad (3)$$

### Algorithm 1 PP-MPI reconstruction based on ADMM

#### Variables

$n$ : iteration index

$\mathbf{x}_n$ : reconstructed image

$\mathbf{z}_n^{(i)}$ : splitting variables;  $\mathbf{d}_n^{(i)}$ : Lagrange multipliers

$f_{PP}$ : proximal mapping for denoising network

$\Psi_{1_{E(\epsilon, I, b)}}$ : proximal mapping for data consistency

**Initialize**  $\mathbf{z}_0^{(i)}$  and  $\mathbf{d}_0^{(i)}$  for  $i = 0, 1$ , set  $n \leftarrow 0$

**while** Stopping criterion is not satisfied **do**

$$\mathbf{x}_{n+1} \leftarrow (\mathbf{I} + \mathbf{A}^T \mathbf{A})^{-1} (\mathbf{A}^T (\mathbf{z}_n^{(0)} + \mathbf{d}_n^{(0)}) + \mathbf{z}_n^{(1)} + \mathbf{d}_n^{(1)})$$

$$\mathbf{z}_{n+1}^{(1)} \leftarrow f_{PP}(\mathbf{x}_{n+1} - \mathbf{d}_n^{(1)})$$

$$\mathbf{d}_{n+1}^{(1)} \leftarrow \mathbf{d}_n^{(1)} + \mathbf{z}_{n+1}^{(1)} - \mathbf{x}_{n+1}$$

$$\mathbf{z}_{n+1}^{(0)} \leftarrow \Psi_{1_{E(\epsilon, I, b)}}(\mathbf{Ax}_{n+1} - \mathbf{d}_n^{(0)})$$

$$\mathbf{d}_{n+1}^{(0)} \leftarrow \mathbf{d}_n^{(0)} + \mathbf{z}_{n+1}^{(0)} - \mathbf{Ax}_{n+1}$$

$$n \leftarrow n + 1$$

**end while**

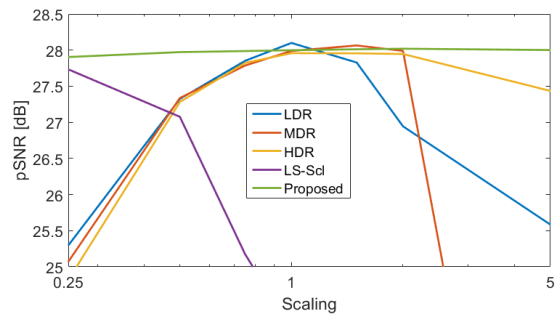


**Figure 1:** pSNR performance of PP-MPI models for test images whose dynamic ranges were scaled in [0.25 5.00] to emulate drifts with respect to training images (i.e., 1 denotes matching scale between training-test images). Results shown for non-scaled models trained on images with varying dynamic ranges (LDR, MDR, HDR), a scaled model based on a least-squares scale estimate (LS-Scl), and the proposed technique.

## III. Methods

In this study, a field-free-line MPI system with a selection field gradient strength of 2.5 T/m was simulated. A sinusoidal drive field with a frequency of 23.2 kHz was used to scan a field of view of  $64 \times 64 \text{ mm}^2$ . Monodisperse MNPs with a diameter of 33.5 nm at 300 °K and a magnetic saturation of  $0.55 \text{ T}/\mu_0$  were used. Finally, an SM of  $64 \times 64$  (1 mm / pixel) size was generated.

To proposed denoiser scaling technique was compared against several baselines. First, non-scaled models were obtained by training the denoiser across images with a broad range of dynamic ranges. To do this, we scaled each image in the training set randomly by a factor of  $\alpha$ . The value of  $\alpha$  was uniformly distributed between  $\alpha \sim U(1, 1)$  for low-dynamic range (LDR),  $\alpha \sim U(0.5, 1.5)$  for mid-dynamic range (MDR) and  $\alpha \sim U(0.1, 5)$  for high dynamic range (HDR), with  $U(a, b)$  denoting the uni-

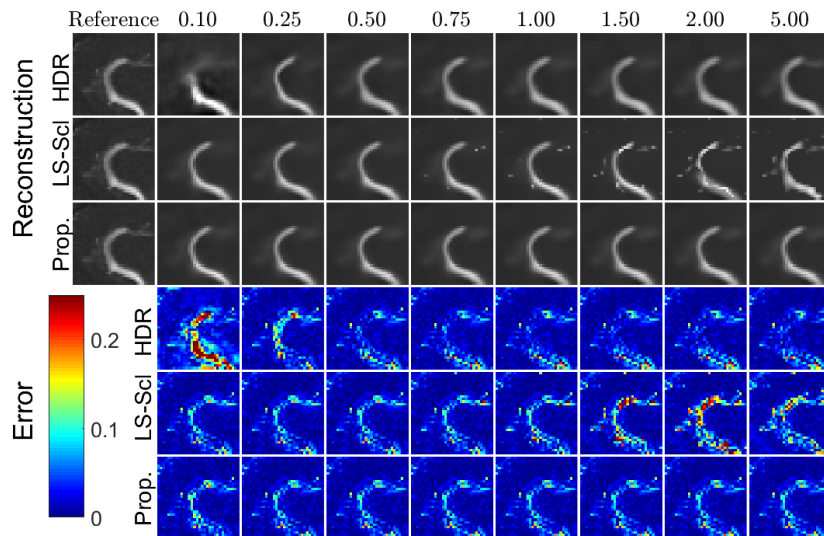


**Figure 2:** Reconstructions of a test phantom along with corresponding error maps for PP-MPI models. HDR is a non-scaled model trained with HDR images, LS-Scl is a scaled model based on a least-squares scale estimate, and Prop. is the proposed denoiser scaling technique. Results are given across drift factors in [0.10 5.00]. The images and error maps are normalized by the drift factor to facilitate comparisons across varying scales. The error map is multiplied by 4 for improved visibility.

formly distributed random variable between  $a$  and  $b$ . Hence, during training, we trained the denoiser to recover  $\alpha \mathbf{x}_i$  from the noisy measurement  $\alpha \mathbf{x}_i + \mathbf{n}_2$ , where  $\mathbf{n}_2$  was an i.i.d. Gaussian noise with a fixed standard deviation of 0.1. Second, a scaled-model was obtained by first estimating the image scale as the peak intensity in an initial least-squares reconstruction [5], and then scaling the denoiser as described in Eq. 3 during all iterations.

For all experiments, we used the MRA dataset and the training procedure described in [9]. To avoid inverse crime, we generated data using the  $64 \times 64$  SM, then reconstructed images on a downsampled SM with size  $32 \times 32$ . Eight separate image reconstructions were performed by emulating scale drifts in the test set by scaling test images with [0.1, 0.25, 0.5, 0.75, 1, 1.5, 2, 5] relative to training images, where 1 corresponds to matched scales between training-test sets. Peak signal-to-noise-ratio (pSNR) was measured on images restored to their original scales:

$$pSNR(\mathbf{x}, \mathbf{x}_{ref}) = 20 \log_{10} \left( \frac{\sqrt{N}}{\|\mathbf{x} - \mathbf{x}_{ref}\|_2} \right), \quad (4)$$

where  $\mathbf{x}_{ref}$  is the reference image and  $N = 1024$  is the number of pixels in the image.

## IV. Results

Figure 1 shows the pSNR performance of PP-MPI models based on non-scaled denoisers trained under varying dynamic ranges (LDR, MDR, HDR), a scaled denoiser where the scale is estimated based on a least-squares

reconstruction, and the proposed two-stage scaled denoiser. Reconstructions were performed for test images whose relative dynamic ranges were altered with a drift factor of [0.25 5.00], where 1 denotes matching dynamic range. Noise was added to attain a data SNR level of 20 dB at each scale. Among non-scaled models, the denoiser trained with HDR images performs favorably, albeit with notable performance losses below a drift factor of 0.50. Meanwhile, given the reconstruction errors in least-squares reconstructions, the least-squares scaled denoiser performs poorly beyond a scaling of 0.50. In comparison, the proposed technique performs reliably across a broad range of drift factors.

Figure 2 displays reconstructions of a representative test phantom along with corresponding error maps. Results are shown of PP-MPI models based on the non-scaled denoiser trained with HDR images that attained relatively higher performance among non-scaled variants, the least-squares scaled denoiser and the proposed two-stage scaled denoiser. Images are displayed for drift factors in [0.10 5.00]. In general, all models tend to perform best at a scaling of 1, with the exception of the least-squares scaling that yields higher errors as the image scaling grows. The non-scaled HDR denoiser suffers from performance loss towards lower drift factors, and the least-squares scaled denoiser performs poorly towards higher drift factors. In contrast, the proposed technique produces high-quality reconstructions across the examined range of drift factors.

## V. Conclusion

Here we presented a denoiser scaling technique to improve reliability of PP-MPI against drift in image scale. We find that non-scaled models trained on HDR images are relatively less sensitive to drifts, but they still show poor performance on test images with LDR. Meanwhile, scaled models based on least-squares yield biased estimates of the image scale due to reconstruction errors, particularly for MDR and HDR images. In contrast, the proposed scaling technique yields robust performance across a broad range of image scales, without requiring any manual tuning. Here we primarily focus on the recent PP-MPI approach, yet our findings and the proposed scaling method can help improve reliability of other learning-based MPI methods against scale drifts.

## Author's statement

Conflict of interest: Authors state no conflict of interest.

## References

- [1] B. Gleich and J. Weizenecker. Tomographic imaging using the nonlinear response of magnetic particles. *Nature*, 435(7046):1214–1217, 2005.
- [2] T. Knopp, J. Rahmer, T. F. Sattel, S. Biederer, J. Weizenecker, B. Gleich, J. Borgert, and T. M. Buzug. Weighted iterative reconstruction for magnetic particle imaging. *Physics in Medicine and Biology*, 55(6):1577–1589, 2010, doi:[10.1088/0031-9155/55/6/003](https://doi.org/10.1088/0031-9155/55/6/003).
- [3] S. Ilbey, C. B. Top, A. Güngör, T. Cukur, E. U. Saritas, and H. E. Güven. Comparison of system-matrix-based and projection-based reconstructions for field free line magnetic particle imaging. *International Journal on Magnetic Particle Imaging*, Vol.3:Article ID 1703022, 2017, doi:[10.18416/IJMPI.2017.1703022](https://doi.org/10.18416/IJMPI.2017.1703022).
- [4] S. Dittmer, T. Kluth, D. O. Baguer, and P. Maass, A deep prior approach to magnetic particle imaging, in *Machine Learning for Medical Image Reconstruction*, Springer International Publishing, 2020, 113–122. doi:[10.1007/978-3-030-61598-7\\_11](https://doi.org/10.1007/978-3-030-61598-7_11).
- [5] A. Güngör, B. Askin, D. A. Soydan, C. B. Top, E. U. Saritas, and T. Çukur, DEQ-MPI: A deep equilibrium reconstruction with learned consistency for magnetic particle imaging, 2022. doi:[10.48550/ARXIV.2212.13233](https://doi.org/10.48550/ARXIV.2212.13233).
- [6] T. Knopp and M. Grosser, Warmstart approach for accelerating deep image prior reconstruction in dynamic tomography, in *MIDL*, 2022.
- [7] B. G. Chae, Neural network image reconstruction for magnetic particle imaging, 2017. doi:[10.48550/ARXIV.1709.07560](https://doi.org/10.48550/ARXIV.1709.07560).
- [8] P. Koch, M. Maass, M. Bruhns, C. Droigk, T. J. Parbs, and A. Mertins, Neural network for reconstruction of MPI images, in *9th International Workshop on Magnetic Particle Imaging*, 39–40, 2019.
- [9] B. Askin, A. Güngör, D. A. Soydan, E. U. Saritas, C. B. Top, and T. Cukur, PP-MPI: A deep plug-and-play prior for magnetic particle imaging reconstruction, in *MLMIR*, 105–114, 2022.
- [10] A. Güngör, B. Askin, D. A. Soydan, E. U. Saritas, C. B. Top, and T. Çukur. TranSMS: Transformers for super-resolution calibration in magnetic particle imaging. *IEEE Transactions on Medical Imaging*, pp. 1–1, 2022, doi:[10.1109/TMI.2022.3189693](https://doi.org/10.1109/TMI.2022.3189693).
- [11] X. Xu, J. Liu, Y. Sun, B. Wohlberg, and U. S. Kamilov, Boosting the performance of plug-and-play priors via denoiser scaling, in *2020 54th Asilomar Conference on Signals, Systems, and Computers*, 1305–1312, 2020. doi:[10.1109/IEEECONF51394.2020.9443410](https://doi.org/10.1109/IEEECONF51394.2020.9443410).